



Published in final edited form as:

J Cogn Neurosci. 2017 July ; 29(7): 1212–1225. doi:10.1162/jocn_a_01112.

Distinct frontoparietal networks underlying attentional effort and cognitive control

Anne S Berry^{1,2}, Martin Sarter^{1,3}, and Cindy Lustig^{1,3}

¹Neuroscience Program, University of Michigan, Ann Arbor, MI

²Lawrence Berkeley National Laboratory, Berkeley, CA

³Psychology Department, University of Michigan, Ann Arbor, MI

Abstract

We investigated the brain activity patterns associated with stabilizing performance during challenges to attention. Our findings revealed distinct patterns of frontoparietal activity and functional connectivity associated with increased attentional effort versus preserved performance during challenged attention. Participants performed a visual signal detection task with and without presentation of a perceptual-attention challenge (changing background). The challenge condition increased activation in frontoparietal regions including right mid-dorsal/dorsolateral prefrontal cortex (RPFC), approximating Brodmann area (BA) 9, and superior parietal cortex. We found that greater behavioral impact of the challenge condition was correlated with greater RPFC activation, suggesting that increased engagement of cognitive control regions is not always sufficient to maintain high levels of performance. Functional connectivity between RPFC and anterior cingulate cortex (ACC) increased during the challenge condition and was also associated with performance declines, suggesting that the level of synchronized engagement of these regions reflects individual differences in attentional effort. Pre-task, resting state RPFC-ACC connectivity did not predict subsequent performance, suggesting that RPFC – ACC connectivity increased dynamically during task performance in response to performance decrement and error feedback. In contrast, functional connectivity between RPFC and superior parietal cortex not only during the task but also during pre-task rest was associated with preserved performance in the challenge condition. Together, these data suggest resting frontoparietal connectivity predicts performance on attention tasks that rely on those same cognitive control networks, and that under challenging conditions, other control regions dynamically couple with this network to initiate the engagement of cognitive control.

INTRODUCTION

Imagine that as you're reading this, your screen or office light is flickering. We hope we've made the paper interesting enough to motivate you to soldier on, but you would undoubtedly find it more challenging. The term "cognitive control" describes the processes engaged to overcome such challenges, and there is increasing interest in the interactions between

cognitive control, motivation, and associated constructs such as “effort” (see review by Botvinick & Braver, 2015). Effort has been defined as the motivated activation of task-set representations in response to reduced performance or other indicators of increased task difficulty due to external or internal factors (e.g., the flickering described above, fatigue, advanced age) (Sarter, Gehring, & Kozak, 2006). The right prefrontal cortex (RPFC) has been proposed as a critical locus for interactions between control, motivation, and effort (e.g., Lustig & Sarter, 2016; Watanabe & Sakagami, 2007). However, as Botvinick and Braver note, the neural correlates of effort remain relatively unexplored. Here, we examined RPFC activation and functional connectivity in a task previously used in rodents to examine the contribution of cortical cholinergic and mesolimbic dopaminergic interactions to attentional effort.

RPFC along middle/inferior frontal gyrus (approximating Brodmann Area (BA) 9) is an important component of the frontoparietal network implicated in control functions including the representation of task goals or rules, biasing activity in functionally connected regions, monitoring the outcome of behavior, and maintaining and updating task representations (reviewed in Dehaene, Kerszberg, & Changeux, 1998; Miller & Cohen, 2001). Supporting the role of BA 9 in directing these functions, it is highly connected with sensory, motor, parietal, and other PFC regions as well as midbrain and limbic structures (Alexander, DeLong, & Strick, 1986; Bates & Goldman-Rakic, 1993; Miller & Cohen, 2001). In a recent review, we noted that it serves as a common locus for increased activation in response to control demands in young adults, putatively compensational increases in activation during control-demanding tasks in older adults, and abnormal function during working memory tasks in schizophrenia (Lustig & Sarter, 2016, their Figure 3).

Across groups and within individuals, BA 9 along right IFG/MFG shows a pattern of initially increased activation in response to increased demand for cognitive control, but decreased activation at higher levels of demand that are associated with performance declines (e.g. Callicott et al., 1998; Cappell, Gmeindl, & Reuter-Lorenz, 2010; Fletcher et al., 1998; Van Snellenberg et al., 2015). This inverted-U pattern may reflect increased recruitment of motivated attention until a “crunch point” (Reuter-Lorenz & Lustig, 2005), after which demand exceeds the subject’s ability to maintain performance. It is not yet clear whether drops in performance and activation reflect loss of motivation, abandoning the current task set to explore alternatives, or some combination of cognitive-motivational processes (Lustig & Sarter, 2016).

St. Peters et al. (2011) examined the contributions of cholinergic and afferent mesolimbic systems to meeting attentional challenge in rodents using the distractor condition sustained attention task (dSAT; McGaughy & Sarter, 1995). The challenge presented by the dSAT is much like that described in our opening sentence: Rapidly-changing background illumination during a signal detection task. As in prior studies indicating the critical role of RPFC cholinergic modulation in responding to attentional challenge, extracellular RPFC acetylcholine (ACh) levels in prefrontal cortex increased during the no-distraction (SAT) condition compared to no-task baseline, and rose further in response to the dSAT challenge (see Sarter, Lustig, Blakely, & Cherian, 2016, for recent review). Furthermore, stimulation of the nucleus accumbens shell – associated with dopaminergic function and “stay on task”

motivation (Floresco, 2015) – improved performance in the dSAT condition. This benefit was specific to the dSAT challenge and did not affect unchallenged (SAT) performance. These beneficial effects depended on an intact cholinergic system: They were eliminated by lesioning either PFC or parietal cholinergic inputs. Together, these results suggest that dopaminergic-motivation and cholinergic-attention systems interact to stabilize performance under challenge.

The RPFC ACh increases seen in rats are paralleled by RPFC activation in human fMRI studies: A small but significant increase in the no-distraction SAT condition compared to no-task baseline, and a further increase (more specific to RPFC) during the dSAT challenge (Berry, Blakely, Sarter, & Lustig, 2015; Demeter, Hernandez-Garcia, Sarter, & Lustig, 2011). These results replicate across samples (college students and community participants age 22–66 yrs) and imaging methods (ASL and BOLD). Increases in RPFC activation during the dSAT correlate with performance, indicating their functional significance (Demeter et al., 2011). However, those correlations were in a counterintuitive direction: Participants with the greatest RPFC increases in response to the dSAT challenge also had the greatest dSAT-related decreases in performance. These results join with those demonstrating RPFC's responsiveness to difficulty across a wide range of tasks and populations (e.g. Chein & Schneider, 2005; Lustig & Sarter, 2016; Rottschy et al., 2012; Turner and Spreng, 2012) to suggest that rather than directly supporting attention, RPFC activation reflects attentional effort (as defined above). This interpretation is further supported by a reverse-inference search of the NeuroSynth database (Yarkoni, Poldrack, Nichols, Van Essen, & Wager, 2011) for the term “task difficulty”, which identifies a right BA 9 cluster spanning middle/inferior frontal gyrus (peak MNI 42, 6, 32, $z = 7.22$) that closely corresponds with results from dSAT (Figure 2a).

The present study had three main goals. The first was to test the replication of our previous results. Both our block design ASL study (Demeter et al., 2011) and event-related BOLD study (Berry et al., 2015) showed RPFC increases in response to the dSAT challenge, but only the former showed the correlation with performance. The relevance of this correlation to the interpretation of RPFC's involvement in attentional effort, as well as general concerns about replication in the field, make crucial to establish whether this discrepancy reflects the change in imaging methods, the smaller and more variable sample in Berry et al., or a false finding in the original study.

Second, we examined the interactions between RPFC and other frontoparietal regions involved in control, and their ability to predict performance. We have hypothesized (Lustig & Sarter, 2016) that RPFC translates demand signals from anterior cingulate (ACC) to the activation and stabilization of the task-set representations needed to meet that demand. If so, greater ACC-RPFC connectivity should be associated with greater dSAT vulnerability, whereas RPFC connections with downstream regions may predict distractor resistance. Third, we tested whether connectivity-performance relations were also present in pre-task resting state data, potentially indicating stable individual differences in the brain networks that support resisting challenges to attention.

METHODS

Participants

18 young adult participants (9 female, mean age = 21.78 yr, range = 18–27 yr) were included in the analysis. All participants were right-handed as determined by the Edinburgh Handedness Scale (Oldfield, 1971), had normal or corrected-to-normal vision, and scored at least a nine on the Extended Range Vocabulary Test (ERVT, Version 3, Educational Testing Services (ETS), 1976; mean score = 20.17, range = 9.00 – 32.25). Participants had no history of psychological or psychiatric disorder, and did not take medications that affect cognition. Data from 2 participants were excluded from analyses of functional runs collected during task performance due to excessive head motion (> 3 mm in x, y, z direction or 3° pitch, roll, yaw). Their resting state scans, collected at the beginning of the fMRI session, were included in the present analysis.

Behavioral task

Participants performed the Sustained Attention Task (SAT) and its distractor condition (dSAT) as previously described (Berry et al., 2015; Demeter et al., 2011; Demeter, Sarter, & Lustig, 2008), implemented using E-prime software (Psychological Software Tools, Pittsburgh, PA). SAT and dSAT trials consisted of signal and nonsignal trials (Figure 1). The signal was a small dark gray square centrally presented for a variable duration (17 – 64 ms). Trials began with a monitoring period (1000, 2000, or 3000 ms; blank light gray screen), at the end of which a signal did (signal event) or did not (nonsignal event) appear. The signal occurred for 50% of the trials. Participants were cued to respond by a 700 ms low-frequency auditory response tone. Participants had up to 1000 ms after the tone to make a keypress response indicating whether or not the signal had been presented on that trial (response-hand mapping was counterbalanced across subjects). A high-frequency tone lasting 700 ms followed correct responses. Responses were classified as hits (correct signal trials), misses (incorrect signal trials), correct rejections (CR; correct nonsignal trials), false alarms (FA; incorrect nonsignal trials), and omissions. dSAT trials were identical to SAT trials except that the background screen alternated between gray and black at 10 Hz. For each task run, participants were paid 1 cent for each percent correct, but penalized 5 cents for the percent of missed trials.

Behavioral analysis

As in prior rodent and human studies, the primary performance measure was SAT score, calculated for each condition (SAT, dSAT) using the formula $SAT\ score = (hits - FAs) / [2(hits + FAs) - (hits + FAs)^2]$. SAT score varies from +1 to -1 with +1 indicating all responses were hits or CRs and -1 indicating all responses were misses or FAs. SAT score was preferred to d' because SAT score does not make assumptions about equal variance of positive and negative responses, which are often violated (see discussion by Frey & Colliver, 1973). Data were analyzed with SPSS, version 21. We assessed the effects of distraction on performance using paired t tests and Cohen's d effect sizes.

fMRI data acquisition and preprocessing

Resting state—Imaging data were collected on a 3 T General Electric Signa scanner with a standard quadrature head coil. Participants used mirrored glasses to view stimuli projected on a screen behind them. Functional images were acquired during rest using a spiral-in sequence with 43 slices and voxel size $3.44 \times 3.44 \times 3$ mm (TR = 2 s, TE = 30 ms, flip angle = 90° , FOV = 22 mm^2). During resting state fMRI acquisition (~ 6 min), a white fixation cross on a black background was displayed in the center of the screen. Participants were asked to remain awake with their eyes open and focused on the cross. Heart rate and respiration were recorded. Resting state scans were acquired in the beginning of the scanning session before task runs. No subject moved more than 0.20 mm in x, y, or z directions or rotated more than 1.57° along pitch, roll, or yaw axes.

Task runs—Each of the six experimental runs contained 75 trials, divided equally among SAT signal, dSAT signal, SAT nonsignal, dSAT nonsignal and fixation (fixation duration 2.2 s – 12.6 s). During fixation the screen alternated between gray and black at 10 Hz. Trials were pseudorandomized to ensure that all possible sequences occurred with equal probability. Prior to functional runs, participants performed in-scanner practice to confirm they remembered task instructions and could clearly hear the response and feedback tones. Practice was repeated until participants reached 60% accuracy.

Functional images were acquired during task performance using a spiral-in sequence with 35 slices and voxel size $3.44 \times 3.44 \times 3$ mm (TR = 2 s, TE = 30 ms, flip angle = 90° , FOV = 22 mm^2). T1-weighted anatomical overlay was acquired in the same functional space (TR = 225 ms, TE = 3.8 ms, flip angle = 90°). A 148-slice high-resolution T1-weighted anatomical image used spoiled-gradient-recalled acquisition (SPGR) in steady-state imaging (TR = 9 ms, TE = 1.8 ms, flip angle = 15° , FOV = 25×26 cm, slice thickness = 1.2 mm).

During preprocessing, structural images were skull-stripped using the Brain Extraction Tool in FSL (FMRIB Software Library; www.fmrib.ox.ac.uk/fsl; Smith et al., 2004) and corrected for signal inhomogeneity. SPGR images were normalized to the Montreal Neurological Institute (MNI) template using SPM 8 (Wellcome Department of Cognitive Neurology, London). To spatially normalize functional images to the MNI template, the functional overlay and SPGR were used as intermediates. All functional images were corrected for differences in slice timing (Oppenheim, Schafer, & Buck, 1999) and head movement using the MCFLIRT algorithm (Jenkinson, Bannister, Brady, & Smith, 2002). Functional images were smoothed with an 8-mm full width/half-maximum isotropic Gaussian kernel and high-pass filtered (128 s).

fMRI univariate analysis

General Linear Model—Data were analyzed using a multisession General Linear Model (GLM) implemented in SPM8. SAT and dSAT hits, CRs, and fixation onsets were modeled as separate predictors. All omissions, misses, and FAs were modeled together as a separate predictor of no interest. Predictors were time-locked to onset of the signal or nonsignal period and convolved with the canonical hemodynamic response function. Six motion regressors derived from individual subject realignment were included in the model.

A priori region of interest analysis—Our lab follows a consistent policy of using *a priori* regions of interest (ROI) to test replication across studies, followed by voxel-wise analyses to examine consistency with the *a priori* results and present a more complete picture of the data. Our *a priori* RPFPC ROI was created on the Demeter et al. (2011) ASL dataset, using the dSAT>SAT>distractor fixation contrast, peak MNI coordinates 35, 9, 33 with a 8mm sphere. Coordinates x, y, z were corrected by -1, -1, -1 to account for origin differences from the ASL analysis. Percent signal-change values for each participant were extracted using MarsBar software (<http://marsbar.sourceforge.net>; Brett, Anton, Valabregue, & Poline, 2002) and subjected to paired *t* tests.

Exploratory whole brain voxel-wise analysis—The more exploratory whole brain voxel-wise analysis used the contrast: dSAT (hits + CRs) > SAT (hits + CRs). This allowed us to examine how closely the data here replicated the peak found in Demeter et al. (2011) despite the different samples, imaging designs, and modality. It also allowed us to focus specifically on challenge-related increases in correct trials (not possible in the Demeter et al. block design). Whole brain analyses used a combined height threshold of $p < .001$, uncorrected and extent threshold of greater than 20 voxels. Regions surviving a false discovery rate (FDR) threshold $p < .01$ are denoted with asterisks in the tables.

The $p < .001$, $k > 20$ threshold is stricter than the $p < .001$, $k > 10$ commonly used in the literature and evaluated by Eklund et al. (2016), but still potentially vulnerable to an inflated false discovery rate. Results not meeting the FDR threshold should be interpreted with caution. To help the reader evaluate the reliability and functional significance of those findings, we report both the overlap with the NeuroSynth “task difficulty” analysis and correlations with behavior. Further, just as we do here and in prior papers for the univariate and behavioral correlation analyses, both univariate and connectivity analyses will be replicated on an independent dataset (Caple et al., in prep.) and results reported even if they are inconsistent with the current findings.

Neural-behavioral correlations—To test whether the present data replicated the activation-performance correlation found in Demeter et al. (2011), we examined the across-participant Pearson correlations between the dSAT-SAT activation increase in the *a priori* ROI and the SAT-dSAT performance decline. To improve sensitivity to individual differences, we also tested the correlation using an 8 mm sphere ROI for each participant centered on their peak voxel (dSAT – SAT) within the *a priori* ROI (henceforth, “individualized *a priori* ROI”).

To test the specificity of the brain-behavior correlation to attentional challenge, we used performance correlations with a control ROI in precuneus, which increases in response to the visual stimulation of the distractor but is not predicted to be specifically involved in responding to attentional challenge. As with the RPFPC ROI, we examined these correlations both for a single 8 mm ROI drawn on the Demeter et al. dataset (peak coordinates 9, -67, 31) and individually-defined ROI within it.

Task-based functional connectivity analysis

Psychophysiological interaction analysis during distractor performance—We have hypothesized that RPFC serves as an important juncture for translating demand signals from ACC to downstream regions involved in implementing more specific control processes (Lustig & Sarter, 2016; see e.g. Wang et al., 2010 for prior work). To test this hypothesis, we generated whole-brain psychophysiological interaction (PPI) (Friston et al., 1997) maps implemented in SPM 8, using a seed region drawn around the peak coordinates of the dSAT > SAT contrast in the current dataset in right inferior frontal gyrus (IFG; 8 mm sphere around MNI 46, 2, 30; hereafter the “study-specific” ROI). Voxels above $p < .05$ for the contrast all task > fixation were excluded from the ROI (henceforth named “study-specific seed”). The first-level model contained separate regressors for the seed region time series, dSAT > SAT contrast, and interaction (the multiplication of the deconvolved BOLD time series from the seed and the contrast regressor). For each subject, voxel-wise PPI effects were estimated, and statistical parametric maps generated for the interaction term. The resulting contrast images were used in second-level PPI group analysis.

Secondary analyses of functional connectivity results: correlation with performance—To determine whether functional connectivity was related to distractor vulnerability or resistance, we tested whether RPFC – ACC connectivity strength correlated with the distractor’s effect on performance and RPFC activation, and which direction. Connectivity values within the significant ACC cluster extracted using the REX toolbox (<http://web.mit.edu/swg/software.htm>), were correlated with the distractor effect (SAT – dSAT score), and percent signal change values (dSAT – SAT) within the study-specific right IFG ROI. Due to the sensitivity of functional connectivity data to motion and the suggestion of one Reviewer, we took additional steps to control for individual differences in motion in all correlation analyses including PPI data. We calculated AFNI’s Euclidian norm of motion parameters ($\|d\|_{L2}$) for each participant and performed partial correlations controlling for mean $\|d\|_{L2}$.

Secondary analyses of functional connectivity results: multiple regression analysis—We next probed the PPI maps specifically for RPFC connections associated with successful distractor resistance. This exploratory voxel-wise regression analysis complemented the correlation analyses described above by identifying pathways that did not necessarily show increased RPFC connectivity when averaged across all subjects, but where individual differences in increased connectivity were associated with individual differences in the ability to maintain performance despite the distractor. Individual PPI interaction contrasts were submitted to second-level regression analyses in SPM with the distractor effect (SAT - dSAT score) entered as a regressor.

Resting state functional connectivity analysis

Pre task functional connectivity—We tested whether pre-task resting-state frontoparietal network activity could predict subsequent attentional performance. Resting state scans were preprocessed as described above. The Euclidian norm ($\|d\|_{L2}$) of motion parameters was calculated for each participant and frames exceeding a threshold of .3 were removed and interpolated using the Artifact Rejection Toolbox (ART; <http://www.nitrc.org/>)

[projects/artifact_detect/](#)) prior to smoothing and normalization. Connectivity analyses were performed using the Functional Connectivity Toolbox version 14.p (CONN; www.nitrc.org/projects/conn; Whitfield-Gabrieli & Nieto-Castanon, 2012). Anatomical images were segmented into gray matter, white matter and CSF to create masks for signal extractions. Regressors of no interest included motion, white matter and CSF. Data underwent linear detrending and were band-pass filtered (0.008 to 0.09 Hz).

Whereas the PPI analyses on the task data asked the question of where the difference between the SAT and dSAT conditions led to increased connectivity, these analyses asked which patterns of variability versus coherence even in the pre-task resting state could predict preserved performance during the dSAT condition (see, e.g., Jimura and Poldrack, 2012 for discussion of interpretation of univariate versus multivariate effects). We first created resting state functional connectivity maps for each participant using the study-specific RPFc ROI centered at 46, 2, 30 as the seed. Next, we performed regression analyses on task data to determine whether patterns of functional connectivity could predict the impact of distraction on performance (SAT – dSAT score) across individuals. We performed targeted analyses of RPFc – ACC connectivity and RPFc – right precuneus/superior parietal lobule (SPL) connectivity based on the PPI regression results, as well as an exploratory whole brain analysis. Masks for ACC and right precuneus/SPL were defined using WFU PickAtlas v3.0 (www.fmri.wfubmc.edu/software/PickAtlas; Lancaster et al., 1997; Lancaster et al., 2000; Maldjian, Laurienti, Kraft, & Burdette, 2003). Regression analyses were conducted using the Pattern Recognition for Neuroimaging Toolbox (PRoNTo) (www.mnl.cs.ucl.ac.uk/pronto; Schrouff et al., 2013). We conducted this analysis using Relevance Vector Regression (RVR; Tipping, 2001) and a leave one subject out cross-validation scheme. Briefly, RVR is a sparse kernel-based machine learning technique that uses Bayesian inference (see Chu, Ni, Tan, Saunders, & Ashburner, 2011 for application to fMRI data). We applied standard procedures in PRoNTo to train the regression model to predict individual participant performance (SAT - dSAT score) based on the patterns of RPFc functional connectivity. To determine the predictive power of RPFc – ACC connectivity, and right RPFc – right precuneus/SPL connectivity individually. ACC and precuneus/SPL masks were specified as features in separate analyses. We report the correlation value between predicted and target (actual) performance for each participant and the mean squared error (MSE). Successful prediction is reflected in positive r values, while positive r values close to zero and negative r values reflect failure of the model to predict the target. Significance levels were calculated for 1,000 permutation tests. The correlation and MSE values for the correctly-paired data were compared to the random 1,000 permutation results reflecting the distribution of correlation and MSE values representing the null hypothesis. Estimated p values for the correlation coefficient were generated by calculating the number of times the correlation r value for randomly paired data was greater than the correlation r value for correctly paired data and dividing by 1,000. Therefore, the reported correlation p values for the RVR analysis do not reflect the p values typically calculated for Pearson correlations.

RESULTS

Behavior

As in previous studies (Berry et al., 2015; Demeter, Guthrie, Taylor, Sarter, & Lustig, 2013; Demeter et al., 2011; Demeter et al., 2008), the dSAT challenge impaired performance. SAT scores were significantly lower in dSAT ($M = .76$, $SD = .15$) relative to SAT ($M = .92$, $SD = .07$), $t(17) = 4.61$, $p < .0001$, $d_z = 1.08$. The hit and FA data from which SAT scores were derived are reported in Table 1.

Univariate analysis

A priori region of interest analysis—In the *a priori* ROI drawn from Demeter et al. (2011), distractor challenge was associated with a marginal trend for greater activation, $t(15) = 1.85$, $p = .08$, $d_z = 0.46$.

Exploratory whole brain voxel-wise analysis—The voxel-wise analyses revealed significant dSAT related increases in RPF activation, although the right inferior frontal gyrus (IFG) peak in the present study (MNI 46, 2, 30) was somewhat posterior to the peak from the Demeter et al. (2011) ASL study (MNI 35, 9, 33). The differences in imaging modality (ASL vs BOLD) and design (block vs event-related) may have contributed to the variation in peak location across studies. Figure 2b shows ROIs from Demeter et al. (2011), the present study, and a previous ASL study that was the basis for the *a priori* ROI tested in Demeter et al. Overall they converge to suggest that RPF (specifically IFG/MFG approximating BA 9) is involved in controlled attention under challenging conditions.

In addition to increasing right IFG activation, dSAT performance was associated with greater activation in other frontoparietal cognitive control regions including right anterior insula/IFG, right superior frontal gyrus/frontal eye fields (FEF), and bilateral superior parietal lobule. (Figure 3, Table 2). Increased activation was also found in cuneus, most likely related to the visual stimulation from the flashing distractor.

Neural-behavioral correlations—We next tested the replication of the correlation between increased RPF activation (dSAT – SAT) and distractor vulnerability in performance (SAT – dSAT) seen in Demeter et al. (2011). Shapiro-Wilk test confirmed the normality of the SAT-dSAT distribution ($W = 0.94$, $p = .29$). As might be expected from the variance in peak location across studies (above), for the *a priori* ROI drawn from Demeter et al., the correlation was in the same direction as in the previous study, but did not meet traditional significance levels, $r = .38$, $p = .15$. To increase sensitivity, we also created individual ROIs for each participant centered on their peak voxel for the dSAT vs SAT contrast within the *a priori* ROI (individualized *a priori* ROIs, see Methods for details). This method allows greater sensitivity in the measurement of each individual's dSAT vs SAT activation contrast, but the ROIs are still defined independently of the correlation (c.f., Vul, Harris, Winkielman, & Pashler, 2009). Using this method, the correlation between distraction-related activation increases and performance decreases was significant, $r = .52$, $p = .04$; see Figure 3.

This correlation pattern was specific to RPFC. Activation increases in the right cuneus *a priori* ROI (see Methods) did not correlate with the behavioral effect (individualized ROIs: $r = -.18$, $p = .50$), indicating that the RPFC correlation was not an artifact of the visual stimulation. To further test the specificity of the right MFG/IFG contribution, we also examined activation-performance correlations for the other frontoparietal regions that increased activation during the dSAT challenge. These did not approach significance (all $r < .28$, $p > .29$) with the exception of right anterior insula/IFG ($r = .49$, $p = .054$). This correlation was driven by a single data point, removal of which lowered the r -value to $.26$. Together, the results suggest the patterns seen in right MFG/IFG were specific to that region.

Task-based functional connectivity

Psychophysiological interaction analysis during distractor performance—Our hypothesis that right MFG/IFG participates in translating error or reward-loss signals from ACC to activation or stabilization of control to respond to attentional challenge (Lustig & Sarter, 2016; Sarter et al., 2006) predicts functional connectivity between these regions. A whole brain voxel-wise analysis of PPI functional connectivity using the study-specific seed found increased functional connectivity for dSAT relative to SAT in ACC, as well as right superior temporal gyrus and right medial frontal gyrus/supplementary motor area, (Figure 4, Table 3). The latter two regions may reflect the representation of the auditory cue and motor response, respectively.

Secondary analyses of functional connectivity results: correlation with performance—If ACC - RPFC connectivity is related to the communication of error/reward-loss signals, then greater connectivity might be found for those individuals who had the largest dSAT-related performance declines. Conversely, if it supports the implementation of specific control processes, then individuals with greater connectivity should have smaller challenge-induced performance declines. Our results were more consistent with the first hypothesis, with a marginal correlation between increased functional connectivity and decreased performance during the dSAT ($r = .48$, $p = .07$; Figure 4). Stronger ACC - RPFC connectivity during dSAT was also correlated with greater enhancement of RPFC activation ($r = .55$, $p = .03$). Supporting the specific involvement of ACC - RPFC connectivity in responding to challenge, RPFC connectivity with medial frontal gyrus/supplementary motor area and superior temporal gyrus did not correlate with performance or RPFC activation, all $r < .35$, $p > .21$.

Secondary analyses of functional connectivity results: multiple regression analysis—Exploratory voxel-wise regression analyses probing connectivity positively related to distractor resistance identified functional connectivity between RPFC and right precuneus/SPL (MNI 20, -68, 48) approximating BA 7 that was strongest for individuals least affected by distraction (Figure 5, Table 3).

Resting state functional connectivity

Pre task functional connectivity—The study-specific RPFC ROI also showed significant functional connectivity with other task-positive frontoparietal regions including superior and inferior parietal lobe, precuneus, cingulate cortex, and superior frontal gyrus

during the pre-task resting state (Figure 6, Table 3). Targeted analyses revealed that resting connectivity between RPFC – precuneus/SPL predicted preserved performance during the challenge condition ($r = .59$, $p = .006$; $MSE = .02$, $p = .03$), whereas right RPFC – ACC connectivity did not ($r = -.68$, $p = .99$; $MSE = .07$, $p = 1.00$) (Figure 7; see Methods for explanation of r and p value calculation).

DISCUSSION

The present study revealed four major results: First, although the strongest increases were located slightly posterior to our *a priori* ROI, we replicated both the increase in RPFC activation during the dSAT and its association with performance decreases. Second, as predicted, the increased challenge imposed by the dSAT increased RPFC-ACC functional connectivity, which in turn, showed a moderate ($r = .47$) association with performance impairment. In contrast, relatively preserved performance was associated with greater increases in RPFC-parietal connectivity. In addition, multivariate pattern analyses (MVPA) showed that RPFC-parietal connectivity (but not RPFC-ACC connectivity) predicted individual differences in the ability to maintain successful performance in the more challenging dSAT condition (see Jimura & Poldrack, 2012 for further discussion of the interpretation of univariate increases versus stronger prediction using MVPA). Together, these findings implicate RPFC as an important component in the brain's response to task difficulty, and help elucidate how different components of frontoparietal networks interact to support motivated performance under challenging conditions.

We focus on the RPFC because of its consistent involvement in responding to the dSAT challenge in both human imaging and rodent neurochemical studies (e.g., Apparsundaram, Martinez, Parikh, Kozak, & Sarter, 2005; Berry et al., 2015; Demeter et al., 2011; Martinez & Sarter, 2004), and based on similar studies that showed activity modulation as a function of task demand and reward context (e.g., Jimura, Locke, & Braver, 2010; Lim et al., 2010; Raizada & Poldrack, 2007). Both the present study and the Neurosynth reverse inference analysis of “task difficulty” also show left frontoparietal involvement, although we found only RPFC correlated with behavior. An interesting question for future metanalyses and parametric studies is whether systematic factors (e.g., verbal vs visuospatial stimuli, demands on analytic vs global processing) predict lateralization.

The RPFC is hypothesized to help translate ACC signals of declining performance and potential reward loss to top-down control, that is, to the recruitment and stabilization of task representations, in an effort to mitigate that decline (e.g., Sarter et al., 2006). Consistent with that hypothesis, those subjects who had the largest increases in errors during the dSAT challenge also had the largest increases in RPFC-ACC connectivity. While the data are consistent with this interpretation, it is important to note that the present study was not designed to adjudicate between the many different theoretical perspectives of the ACC's role in cognition (see Ebitz & Hayden (2016) or Heilbronner & Hayden (2016) for recent summaries of some of the major theoretical views). For example, ACC activity has also been connected to arousal (e.g., Critchley et al., 2005; see Schneider, Hathway et al., 2016 NeuroImage for correspondence between changes in pupil dilation and activation of the salience network, including ACC, during resting state). Given the correlational nature of

fMRI data, by such an interpretation of ACC function it is equally possible that ACC-mediated (over)arousal leads to an increase in errors or, conversely, that ACC-mediated arousal increases in response to an increase in errors. Either version of the arousal account of ACC function could predict increased RPFCC connectivity, reflecting either increased top-down control to attempt to reduce overarousal and errors, or as arousal invigorating the recruitment of control.

In contrast to the patterns seen for RPFCC-ACC connectivity, RPFCC-parietal connectivity, while not significant when averaging across all subjects, was increased in those subjects who were better able to preserve performance. This may reflect better recruitment of the parietal processes involved in detecting and responding to the target signal under challenge. This interpretation of these regions' involvement will require further testing, but is consistent with other empirical findings and theoretical perspectives.

For example, modeling work (Botvinick, Braver, Barch, Carter, & Cohen, 2001) has demonstrated that pairing a conflict signal (ACC signal) with adjustments in the allocation of control (PFC signal) can accurately simulate the trial-based adjustments in behavior made by subjects during attentional challenge (Botvinick, Nystrom, Fissell, Carter, & Cohen, 1999; Logan, Zbrodoff, & Fostey, 1983; Tzelgov, Henik, & Berger, 1992). The right precuneus/SPL region identified in our study is commonly considered part of the dorsal attention network involved in the top-down control of attention, especially visuospatial attention (e.g., Corbetta & Shulman, 2002; Dosenbach et al., 2007). Of particular interest, Woldorff et al. (2004) found that superior parietal cortex near the region identified here (MNI coordinates 32, -61, 45) was associated with processing and interpreting visuospatial cues, whereas precuneus was more involved in orienting attention towards the target. Both of these processes should be important to successful performance in the signal detection task used here.

In addition to the difference in the direction of RPFCC-ACC vs RPFCC-parietal connectivity associations with performance under challenge, the differences in the stability of that relationship are also consistent with their hypothesized roles. Both regions showed significant connectivity with the RPFCC region during rest, but only parietal connectivity predicted performance. The failure of RPFCC-ACC rest-state connectivity to predict performance may reflect that ACC signals of error reward loss are common across many situations rather than being specifically related to challenged signal detection. Further, those signals may only become relevant during task performance, i.e., when errors occur. In contrast, processing and orienting to signals, supported by superior parietal/precuneus involvement, has a more specific role in signal detection. That is, RPFCC-parietal rest-state connectivity may reflect the efficiency of the pathways supporting recruitment of detection processes. Although we did not directly test the long-term stability of the association, rest-state connectivity between these regions has been linked to structural connectivity via the superior longitudinal fasciculus (van den Heuvel, Stam, Kahn, & Hulshoff Pol, 2009), and individual differences in resting frontoparietal connectivity have been demonstrated to remain consistent across sessions and to be predictive of cognitive performance (Finn et al., 2015). RPFCC-parietal connectivity thus has potential as a stable marker of the ability to maintain signal detection under challenge.

While RPF-ACC connectivity may play a more general role across tasks than parietal involvement, this does not entail that it would increase with all forms of attentional challenge. There is still significant controversy about the exact role of the ACC in cognition, but general agreement that it is responsive to feedback and reward potential (e.g., Alexander & Brown, 2015; Euston, Gruber, & McNaughton, 2012; Shenhav, Botvinick, & Cohen, 2013; Silvetti, Seurinck, & Verguts, 2011). Our discussion has emphasized the potential for reward loss in keeping with the idea of “challenge”, but potential gain would be expected to have similar effects. In contrast, when challenge was manipulated by unpredictably varying the difficulty of making sensory judgments, and no feedback was offered, Raizada and Poldrack (2007) identified a RPF region very similar to the one found here, but with connectivity to the locus coeruleus (LC) rather than ACC. They suggested that while RPF may play a common role in allocating cognitive resources, its connectivity varies depending on whether the task situation emphasizes potential reward loss/gain (ACC and cholinergic modulation) versus unpredictability (LC and noradrenergic modulation). An earlier rodent study provides some support for this interpretation: Dalley et al. (2001) found that extracellular cortical ACh levels increased when reward was based on task performance, but noradrenaline levels increased when task conditions changed so that reward was unpredictable.

Together these studies suggest a heuristic framework for RPF involvement in dealing with challenging situations: RPF-ACC interactions invoke cholinergically-mediated recruitment and stabilization of task representations to promote the gain of/prevent the loss of expected rewards, whereas RPF-LC interactions play a complementary role in promoting noradrenergically-mediated flexibility in representations when the environment is unpredictable. A third, potentially dopaminergic, piece to the attentional effort puzzle is suggested by the findings of Jimura et al. (2010). They found that the dynamics of RPF engagement – whether it was engaged in a more sustained, early manner consistent with proactive control versus a late, transient response associated with reactive control – depended on whether or not reward was offered and individual sensitivity to reward. They suggested that transient midbrain dopamine signals might provoke the activation of sustained frontoparietal control mechanisms. This suggestion receives indirect support from the nucleus accumbens-basal forebrain-frontoparietal interactions reported by St. Peters et al. (2011). Altogether, these studies suggest that RPF plays a critical role in integrating the cortical and subcortical systems that mediate attentional effort and cognitive control.

Fully testing the RPF’s role as a hub for the interaction of systems mediating the top-down reinforcement of current goals, flexibility in those goals in face of change or unpredictability, and the motivation to respond to challenge would require a series of studies parametrically manipulating those dimensions. The present study establishes the replicability of its response to an attentional challenge and its correlation with behavior, and suggests pathways by which it may be involved in translating the need for control into its engagement. It thus takes a more modest but important step in elucidating the neural components that support performance in the face of attentional challenge.

Acknowledgments

Funding

This research was supported by PHS grants R01MH086530 (MS, CL), and by a grant from the National Science Foundation (0726285, CL). Anne Berry was supported by a NSF Graduate Research Fellowship.

References

- Alexander &, Brown JW. Hierarchical Error Representation: A Computational Model of Anterior Cingulate and Dorsolateral Prefrontal Cortex. *Neural Comput.* 2015; 27(11):2354–2410. [PubMed: 26378874]
- Alexander, DeLong MR, Strick PL. Parallel organization of functionally segregated circuits linking basal ganglia and cortex. *Annu Rev Neurosci.* 1986; 9:357–381. [PubMed: 3085570]
- Apparsundaram S, Martinez V, Parikh V, Kozak R, Sarter M. Increased capacity and density of choline transporters situated in synaptic membranes of the right medial prefrontal cortex of attentional task-performing rats. *J Neurosci.* 2005; 25(15):3851–3856. [PubMed: 15829637]
- Bates JF, Goldman-Rakic PS. Prefrontal connections of medial motor areas in the rhesus monkey. *J Comp Neurol.* 1993; 336(2):211–228. [PubMed: 7503997]
- Berry AS, Blakely RD, Sarter M, Lustig C. Cholinergic capacity mediates prefrontal engagement during challenges to attention: evidence from imaging genetics. *Neuroimage.* 2015; 108:386–395. [PubMed: 25536497]
- Botvinick &, Braver T. Motivation and cognitive control: from behavior to neural mechanism. *Annu Rev Psychol.* 2015; 66:83–113. [PubMed: 25251491]
- Botvinick Braver TS, Barch DM, Carter CS, Cohen JD. Conflict monitoring and cognitive control. *Psychol Rev.* 2001; 108(3):624–652. [PubMed: 11488380]
- Botvinick Nystrom LE, Fissell K, Carter CS, Cohen JD. Conflict monitoring versus selection-for-action in anterior cingulate cortex. *Nature.* 1999; 402(6758):179–181. [PubMed: 10647008]
- Brett, M., Anton, J., Valabregue, R., Poline, J. Region of interest analysis using an SPM toolbox [abstract]. Paper presented at the 8th International Conference on Functional Mapping of the Human Brain; 2002.
- Callicott JH, Ramsey NF, Tallent K, Bertolino A, Knable MB, Coppola R, et al. Functional magnetic resonance imaging brain mapping in psychiatry: methodological issues illustrated in a study of working memory in schizophrenia. *Neuropsychopharmacology.* 1998; 18(3):186–196. [PubMed: 9471116]
- Cappell KA, Gmeindl L, Reuter-Lorenz PA. Age differences in prefrontal recruitment during verbal working memory maintenance depend on memory load. *Cortex.* 2010; 46(4):462–473. [PubMed: 20097332]
- Chein JM, Schneider W. Neuroimaging studies of practice-related change: fMRI and meta-analytic evidence of a domain-general control network for learning. *Brain Res Cogn Brain Res.* 2005; 25(3):607–623. [PubMed: 16242923]
- Chu C, Ni Y, Tan G, Saunders CJ, Ashburner J. Kernel regression for fMRI pattern prediction. *Neuroimage.* 2011; 56(2):662–673. [PubMed: 20348000]
- Corbetta M, Shulman GL. Control of goal-directed and stimulus-driven attention in the brain. *Nat Rev Neurosci.* 2002; 3(3):201–215. [PubMed: 11994752]
- Critchley HD, Tang J, Glaser D, Butterworth B, Dolan RJ. Anterior cingulate activity during error and autonomic response. *NeuroImage.* 2005; 27:885–895. [PubMed: 15996878]
- Dalley JW, McGaughy J, O’Connell MT, Cardinal RN, Levita L, Robbins TW. Distinct changes in cortical acetylcholine and noradrenaline efflux during contingent and noncontingent performance of a visual attentional task. *J Neurosci.* 2001; 21(13):4908–4914. [PubMed: 11425918]
- Dehaene S, Kerszberg M, Changeux JP. A neuronal model of a global workspace in effortful cognitive tasks. *Proc Natl Acad Sci U S A.* 1998; 95(24):14529–14534. [PubMed: 9826734]

- Demeter E, Guthrie SK, Taylor SF, Sarter M, Lustig C. Increased distractor vulnerability but preserved vigilance in patients with schizophrenia: evidence from a translational Sustained Attention Task. *Schizophr Res*. 2013; 144(1–3):136–141. [PubMed: 23374860]
- Demeter E, Hernandez-Garcia L, Sarter M, Lustig C. Challenges to attention: a continuous arterial spin labeling (ASL) study of the effects of distraction on sustained attention. *Neuroimage*. 2011; 54(2): 1518–1529. [PubMed: 20851189]
- Demeter E, Sarter M, Lustig C. Rats and humans paying attention: cross-species task development for translational research. *Neuropsychology*. 2008; 22(6):787–799. [PubMed: 18999353]
- Dosenbach NU, Fair DA, Miezin FM, Cohen AL, Wenger KK, Dosenbach RA, et al. Distinct brain networks for adaptive and stable task control in humans. *Proc Natl Acad Sci U S A*. 2007; 104(26):11073–11078. [PubMed: 17576922]
- Ebitz RB, Hayden BY. Dorsal anterior cingulate: A Rorschach test for cognitive Neuroscience. *Nature Neuroscience*. 2016; 19:1278–1279. [PubMed: 27669987]
- Eklund A, Nichols TE, Knutsson H. Cluster failure: Why fMRI inferences for spatial extent have inflated false-positive rates. *Proceedings of the National Academy of Sciences USA*. 2016; 113:7900–7905.
- Euston DR, Gruber AJ, McNaughton BL. The role of medial prefrontal cortex in memory and decision making. *Neuron*. 2012; 76(6):1057–1070. [PubMed: 23259943]
- Finn ES, Shen X, Scheinost D, Rosenberg MD, Huang J, Chun MM, et al. Functional connectome fingerprinting: identifying individuals using patterns of brain connectivity. *Nat Neurosci*. 2015; 18(11):1664–1671. [PubMed: 26457551]
- Fletcher PC, McKenna PJ, Frith CD, Grasby PM, Friston KJ, Dolan RJ. Brain activations in schizophrenia during a graded memory task studied with functional neuroimaging. *Arch Gen Psychiatry*. 1998; 55(11):1001–1008. [PubMed: 9819069]
- Floresco SB. The nucleus accumbens: an interface between cognition, emotion, and action. *Annu Rev Psychol*. 2015; 66:25–52. [PubMed: 25251489]
- Frey PW, Colliver JA. Sensitivity and responsivity measures for discrimination learning. *Learning and Motivation*. 1973; 4:327–342.
- Friston KJ, Buechel C, Fink GR, Morris J, Rolls E, Dolan RJ. Psychophysiological and modulatory interactions in neuroimaging. *Neuroimage*. 1997; 6(3):218–229. [PubMed: 9344826]
- Jenkinson M, Bannister P, Brady M, Smith S. Improved optimization for the robust and accurate linear registration and motion correction of brain images. *Neuroimage*. 2002; 17(2):825–841. [PubMed: 12377157]
- Jimura K, Locke HS, Braver TS. Prefrontal cortex mediation of cognitive enhancement in rewarding motivational contexts. *Proc Natl Acad Sci U S A*. 2010; 107(19):8871–8876. [PubMed: 20421489]
- Jimura K, Poldrack R. Analyses of regional-average activation and multivoxel pattern information tell complementary stories. *Neuropsychologia*. 2012; 50:544–552. [PubMed: 22100534]
- Heilbronner SR, Hayden BY. Dorsal anterior cingulate: A bottom-up view. *Annual Review of Neuroscience*. 2016; 39:149–170.
- Lancaster JL, Rainey LH, Summerlin JL, Freitas CS, Fox PT, Evans AC, et al. Automated labeling of the human brain: a preliminary report on the development and evaluation of a forward-transform method. *Hum Brain Mapp*. 1997; 5(4):238–242. [PubMed: 20408222]
- Lancaster JL, Woldorff MG, Parsons LM, Liotti M, Freitas CS, Rainey L, et al. Automated Talairach atlas labels for functional brain mapping. *Hum Brain Mapp*. 2000; 10(3):120–131. [PubMed: 10912591]
- Lim J, Wu WC, Wang J, Detre JA, Dinges DF, Rao H. Imaging brain fatigue from sustained mental workload: an ASL perfusion study of the time-on-task effect. *Neuroimage*. 2010; 49(4):3426–3435. [PubMed: 19925871]
- Logan GD, Zbrodoff NJ, Fostey AR. Costs and benefits of strategy construction in a speeded discrimination task. *Memory & cognition*. 1983; 11(5):485–493. [PubMed: 6419009]
- Lustig C, Sarter M. Attention and the cholinergic system: Relevance to schizophrenia. *Curr Top in Behav Neurosci*. 2016; 28:327–362.

- Maldjian JA, Laurienti PJ, Kraft RA, Burdette JH. An automated method for neuroanatomic and cytoarchitectonic atlas-based interrogation of fMRI data sets. *Neuroimage*. 2003; 19(3):1233–1239. [PubMed: 12880848]
- Martinez V, Sarter M. Lateralized attentional functions of cortical cholinergic inputs. *Behav Neurosci*. 2004; 118(5):984–991. [PubMed: 15506881]
- McGaughy J, Sarter M. Behavioral vigilance in rats: task validation and effects of age, amphetamine, and benzodiazepine receptor ligands. *Psychopharmacology*. 1995; 117(3):340–357. [PubMed: 7770610]
- Miller EK, Cohen JD. An integrative theory of prefrontal cortex function. *Annu Rev Neurosci*. 2001; 24:167–202. [PubMed: 11283309]
- Oldfield RC. The assessment and analysis of handedness: the Edinburgh inventory. *Neuropsychologia*. 1971; 9(1):97–113. [PubMed: 5146491]
- Oppenheim, AV., Schafer, RW., Buck, JR. *Discrete-time signal processing*. Englewood Cliffs, NJ: Prentice Hall; 1999.
- Raizada RD, Poldrack RA. Challenge-driven attention: interacting frontal and brainstem systems. *Front Hum Neurosci*. 2007; 1:3. [PubMed: 18958217]
- Reuter-Lorenz PA, Lustig C. Brain aging: reorganizing discoveries about the aging mind. *Curr Opin Neurobiol*. 2005; 15(2):245–251. [PubMed: 15831410]
- Rottschy C, Langner R, Dogan I, Reetz K, Laird AR, Schulz JB, et al. Modelling neural correlates of working memory: a coordinate-based meta-analysis. *Neuroimage*. 2012; 60(1):830–846. [PubMed: 22178808]
- Sarter M, Gehring WJ, Kozak R. More attention must be paid: the neurobiology of attentional effort. *Brain Res Rev*. 2006; 51(2):145–160. [PubMed: 16530842]
- Sarter M, Lustig C, Blakely RD, Cherian AK. Cholinergic genetics of visual attention: human and mouse choline transporter capacity variants influence distractibility. *Journal of Physiology - Paris*. 2016
- Schneider M, Hathway P, Leuchs L, Samann PG, Czisch M, Spoormaker VI. Spontaneous pupil dilations during the resting state are associated with the activation of the salience network. *NeuroImage*. 2016; 139:189–201. [PubMed: 27291493]
- Schrouff J, Rosa MJ, Rondina JM, Marquand AF, Chu C, Ashburner J, et al. PRoNTTo: pattern recognition for neuroimaging toolbox. *Neuroinformatics*. 2013; 11(3):319–337. [PubMed: 23417655]
- Shenhav A, Botvinick MM, Cohen JD. The expected value of control: an integrative theory of anterior cingulate cortex function. *Neuron*. 2013; 79(2):217–240. [PubMed: 23889930]
- Silvetti M, Seurinck R, Verguts T. Value and prediction error in medial frontal cortex: integrating the single-unit and systems levels of analysis. *Front Hum Neurosci*. 2011; 5:75. [PubMed: 21886616]
- Smith SM, Jenkinson M, Woolrich MW, Beckmann CF, Behrens TE, Johansen-Berg H, et al. Advances in functional and structural MR image analysis and implementation as FSL. *Neuroimage*. 2004; 23(Suppl 1):S208–219. [PubMed: 15501092]
- St Peters M, Demeter E, Lustig C, Bruno JP, Sarter M. Enhanced control of attention by stimulating mesolimbic-corticothalamic cholinergic circuitry. *Journal of Neuroscience*. 2011; 31:9760–9771. [PubMed: 21715641]
- Tipping ME. Sparse bayesian learning and the relevance vector machine. *Journal of Machine Learning Research*. 2001; 1:211–244.
- Turner GR, Spreng RN. Executive functions and neurocognitive aging: dissociable patterns of brain activity. *Neurobiol Aging*. 2012; 33(4):826.e821–813.
- Tzelgov J, Henik A, Berger J. Controlling Stroop effects by manipulating expectations for color words. *Memory & cognition*. 1992; 20(6):727–735. [PubMed: 1435275]
- van den Heuvel MP, Stam CJ, Kahn RS, Hulshoff Pol HE. Efficiency of functional brain networks and intellectual performance. *J Neurosci*. 2009; 29(23):7619–7624. [PubMed: 19515930]
- Van Snellenberg JX, Slifstein M, Read C, Weber J, Thompson JL, Wager TD, et al. Dynamic shifts in brain network activation during supracapacity working memory task performance. *Hum Brain Mapp*. 2015; 36(4):1245–1264. [PubMed: 25422039]

- Vul E, Harris C, Winkielman P, Pashler H. Puzzlingly high correlations in fMRI studies of emotion, personality, and social cognition. *Perspectives on Psychological Science*. 2009; 4:274–290. [PubMed: 26158964]
- Wang L, Liu X, Guise KG, Knight RT, Ghajar J, Fan J. Effective connectivity of the fronto-parietal network during attentional control. *J Cogn Neurosci*. 2010; 22(3):543–553. [PubMed: 19301995]
- Watanabe M, Sakagami M. Integration of cognitive and motivational context information in the primate prefrontal cortex. *Cereb Cortex*. 2007; 17(Suppl 1):i101–109. [PubMed: 17725993]
- Whitfield-Gabrieli S, Nieto-Castanon A. Conn: a functional connectivity toolbox for correlated and anticorrelated brain networks. *Brain Connect*. 2012; 2(3):125–141. [PubMed: 22642651]
- Woldorff MG, Hazlett CJ, Fichtenholtz HM, Weissman DH, Dale AM, Song AW. Functional parcellation of attentional control regions in the human brain. *Journal of Cognitive Neuroscience*. 2004; 16:149–165. [PubMed: 15006044]
- Yarkoni T, Poldrack RA, Nichols TE, Van Essen DC, Wager TD. Large-scale automated synthesis of human functional neuroimaging data. *Nat Methods*. 2011; 8(8):665–670. [PubMed: 21706013]

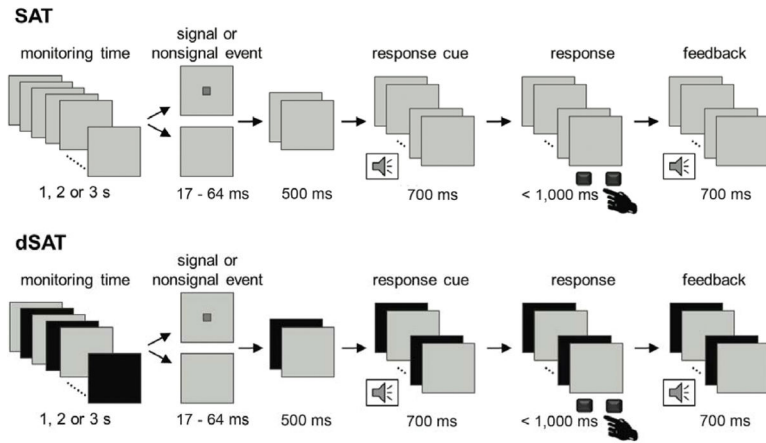


Figure 1. Sustained Attention Task (SAT)

Each trial consisted of a variable duration monitoring interval followed by the presentation of a signal or nonsignal event. The signal was a gray square on a silver background and varied in duration. Signal and nonsignal events were pseudorandomized and occurred with equal frequency. After the auditory cue, participants responded via buttonpress using one index finger for signal trials and the other index finger for nonsignal trials (left-right key assignment counterbalanced across participants). Correct responses were followed by a high frequency feedback tone; incorrect responses or omissions did not result in feedback. The distractor condition, dSAT, increased the attentional control demands of the task by adding a global, continuous visual distractor. During dSAT trials, the screen alternated between gray and black at 10 Hz. SAT, dSAT, and fixation (not pictured) trials were pseudorandomly intermixed.

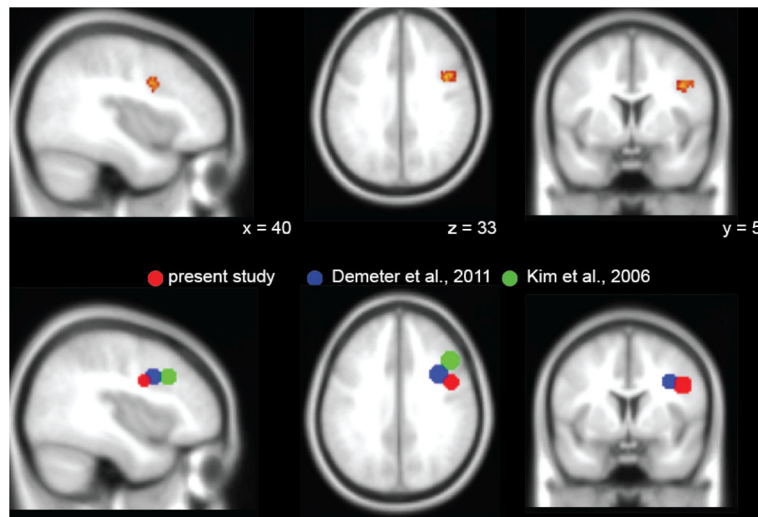


Figure 2. Comparison of right BA 9 peak activations across studies

(a) Reverse-inference analysis of the term “task difficulty” in NeuroSynth revealed a right BA 9 cluster (MNI 42, 6, 32, $z = 7.22$) spanning middle/inferior frontal gyrus at $p < .01$, False Discovery Rate corrected. A cluster threshold of 150 voxels was applied for display purposes to highlight the right lateral prefrontal cortex activation. ROIs are displayed on an SPM template average of 152 normalized T1 anatomical scans. (b) Regions of interest (8 mm spheres) were drawn to surround the peak activation in right BA 9 for the present study (MNI 46, 2, 30), Demeter et al. (2011) (MNI 35, 9, 33), and Kim et al. (2006) (MNI 45, 21, 33). Though the imaging modality (BOLD vs ASL) and design (block vs event-related) varied across study, the findings generally converge to suggest a role of right BA 9 (specifically IFG/MFG) in controlled attention under challenging conditions.

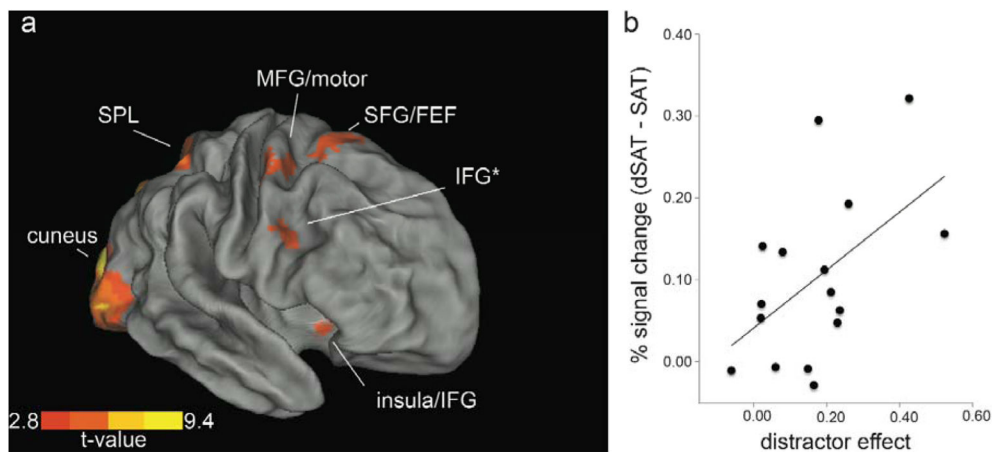


Figure 3. Univariate activation for distractor challenge and neural-behavioral correlation

(a) The contrast $dSAT > SAT$ revealed activation in regions associated with cognitive control and top-down modulation of attentional orienting. Activation in right inferior frontal gyrus (IFG) approximating BA 9, highlighted with an asterisk, generally replicated our previous ASL findings (Demeter et al., 2011). The peak coordinates for this IFG region were used to define the seed region for subsequent functional connectivity analyses. Enhanced activation during distractor challenge was also found in superior parietal lobule (SPL), middle frontal gyrus (MFG), superior frontal gyrus (SFG)/frontal eye fields (FEF), anterior insula, and cuneus. The t-map is displayed on CARET slightly inflated surface representation at a slightly reduced threshold to aid in the visualization of activations at the cortical surface ($p < .05$, FDR corrected). (b) There was a correlation between enhanced BA 9 activation ($dSAT - SAT$) and the distractor effect on performance ($SAT - dSAT$ score), $r = .52$, $p = .04$. Increased right BA 9 activation was measured from individualized ROIs based on the *a priori* region of interest identified in Demeter et al., 2011 and replicated previous findings that participants with the greatest performance decrements during $dSAT$ showed the greatest increase in activation.

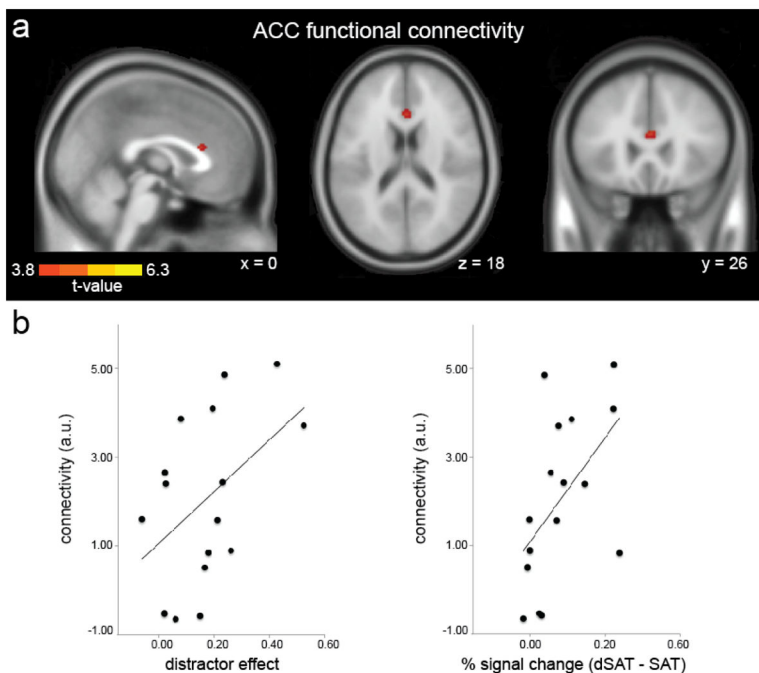


Figure 4. PPI functional connectivity during distractor challenge

(a) Psychophysiological interaction (PPI) analyses revealed greater functional connectivity between the right PFC (RPFC) seed region (8 mm sphere centered on IFG peak coordinates MNI 46, 2, 30) and anterior cingulate cortex (ACC) during distractor challenge. RPFC also showed increased connectivity with regions listed in Table 3, medial frontal gyrus/ supplementary motor area and superior temporal gyrus (not displayed). T-maps are displayed on an SPM template average of 152 normalized T1 anatomical scans, $p < .001$, $k > 20$ (see Methods). (b) Increased right ACC - RPFC functional connectivity (arbitrary units, a.u.) was associated with greater performance declines during distractor challenge and greater increases in right RPFC activation. Functional connectivity strength showed a modest relationship between the distractor effect on performance (SAT - dSAT score), $r = .48$, $p = .07$, and increased RPFC activation, $r = .55$, $p = .03$.

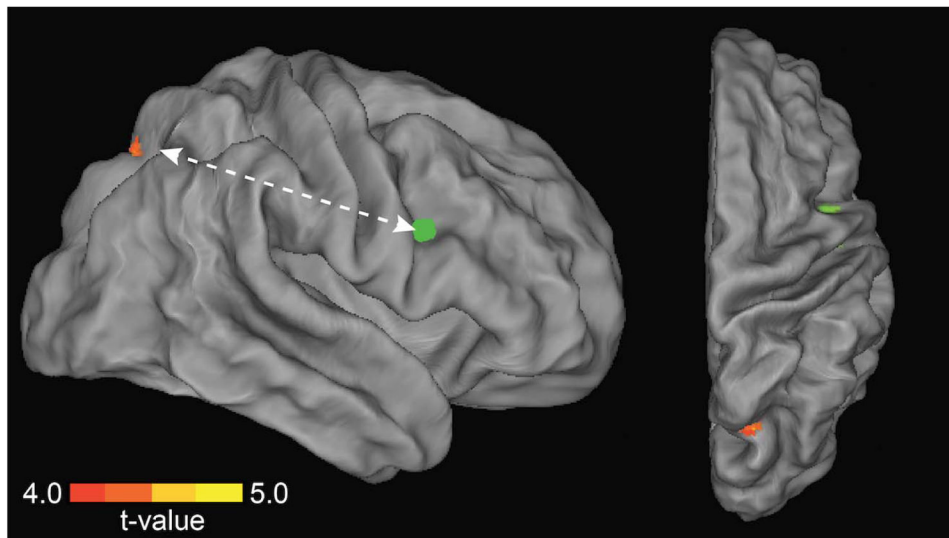


Figure 5. Frontoparietal functional connectivity associated with preserved performance during distractor challenge

Multivariate regression analyses identified a region in right precuneus/superior parietal lobule (SPL, warm colors) whose functional connectivity with right PFC (8 mm sphere centered on inferior frontal gyrus peak coordinates MNI 46, 2, 30) was greatest for individuals with low behavioral impact of distraction. Green indicates the location of the seed.

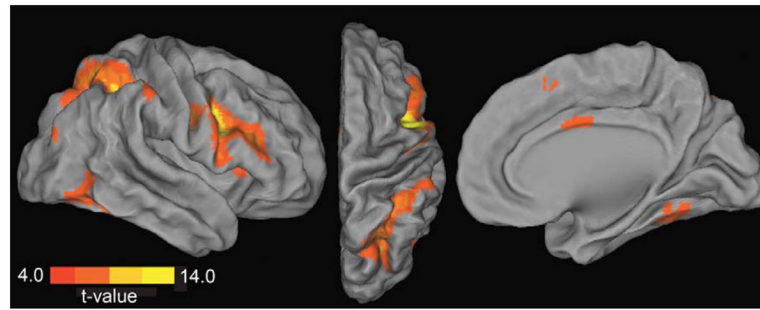


Figure 6. Resting state functional connectivity before task performance

Regions showing positive synchronization with the right PFC seed region (8 mm sphere centered on inferior frontal gyrus peak coordinates MNI 46, 2, 30) during the resting state scan collected prior to task performance are displayed. Activity in right PFC was correlated with other task positive regions including superior and inferior parietal cortex, middle frontal gyrus, inferior temporal gyrus (lateral and dorsal views), and cingulate cortex (medial view). Displayed activations are at $p < .001$, $k > 20$; see Table 3 for FDR correction.

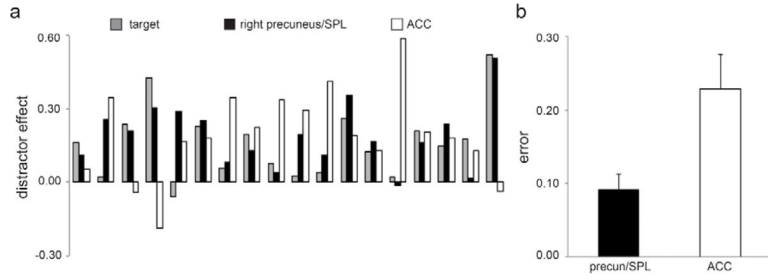


Figure 7. Resting frontoparietal connectivity predicts behavioral distractor effect
 A relevance vector regression model significantly predicted subsequent task performance (SAT – dSAT score) based on patterns of connectivity between the right PFC seed region (8 mm sphere centered on IFG peak coordinates MNI 46, 2, 30) and right precuneus/superior parietal lobule (SPL), but not anterior cingulate cortex (ACC). Parietal and ACC masks were structurally defined. (a) Results for individual participants. Grey bars (“target”) show the magnitude of the actual performance distractor effect (SAT score – dSAT score); black bars show the predicted score when RPFC connectivity with right precuneus/SPL is used as the predictor; white bars show the predicted score when RPFC connectivity with ACC is used as the predictor. (b) Average model error (difference between predicted and actual score) was relatively small when RPFC-right precuneus/SPL connectivity was used as the predictor, and over twice as large when RPFC-ACC connectivity was used as the predictor.

Author Manuscript

Author Manuscript

Author Manuscript

Author Manuscript

Table 1
Hit, false alarm, and omission proportions for SAT and dSAT trials

Data are means (standard deviation around the mean).

| | Hits | False Alarms | Omissions |
|------|-------------|---------------------|------------------|
| SAT | .93 (.05) | .02 (.02) | .02 (.05) |
| dSAT | .80 (.12) | .06 (.06) | .03 (.06) |

Author Manuscript

Author Manuscript

Author Manuscript

Author Manuscript

Univariate results

List of regions showing a significant activation applying a height threshold of $p < .001$ uncorrected, and a cluster volume threshold of greater than 20 voxels. Regions surviving voxel-wise false discovery rate correction $p < .01$ are marked with an asterisk (*). Clusters overlapping with NeuroSynth reverse-inference meta-analysis of “task difficulty” (139 studies) are marked with a †

Table 2

| Size (voxels) | Anatomical label | BA | MINI coordinates | T-score |
|----------------------|--|----|------------------|---------|
| dSAT > SAT | | | | |
| 15453 | cuneus* | 18 | -2 -80 6 | 10.71 |
| 337 | left superior parietal lobule* | 7 | -28 -56 60 | 6.77 |
| 176 | right superior parietal lobule*† | 7 | 26 -56 52 | 6.36 |
| 135 | right superior frontal gyrus/frontal eye fields* | 6 | 12 6 58 | 6.42 |
| 111 | left middle frontal gyrus*† | 6 | -30 -2 54 | 5.41 |
| 53 | right middle frontal gyrus*† | 6 | 38 -6 50 | 4.89 |
| 64 | right inferior frontal gyrus*† | 9 | 46 2 30 | 4.41 |
| 31 | right insula/inferior frontal gyrus*† | 47 | 32 16 -12 | 4.01 |

SAT > dSAT

No significant clusters

Multivariate results

List of regions showing significant functional connectivity applying a height threshold of $p < .001$ uncorrected, cluster volume threshold greater than 20 voxels. Regions surviving voxel-wise false discovery rate correction $p < .01$ are marked with an asterisk. Clusters overlapping with NeuroSynth reverse-inference meta-analysis of “task difficulty” (139 studies) are marked with a †

Table 3

| Size (voxels) | Anatomical label | MNI coordinates | | | T- score | |
|--|---|-----------------|-----|-----|----------|-------|
| | | BA | x | y | | z |
| PPI: dSAT > SAT | | | | | | |
| 50 | right medial frontal gyrus | 6 | 14 | -2 | 56 | 6.34 |
| 25 | right superior temporal gyrus | 41 | 46 | -22 | 10 | 4.88 |
| 23 | anterior cingulate gyrus | 24 | 0 | 24 | 16 | 4.41 |
| PPI: dSAT > SAT regression | | | | | | |
| 69 | right precuneus/superior parietal lobule† | 7 | 20 | -68 | 48 | 4.74 |
| BA 9 resting state connectivity | | | | | | |
| 4410 | right inferior frontal/precentral gyrus*† | 6/9 | 44 | 2 | 32 | 30.50 |
| 5779 | right precuneus/superior and inferior parietal lobe*† | 7 | 28 | -54 | 50 | 13.14 |
| 2699 | left inferior frontal gyrus/precentral gyrus*† | 6/9 | -48 | 2 | 32 | 12.55 |
| 2779 | left precuneus/superior and inferior parietal lobe*† | 7 | -30 | -50 | 50 | 11.01 |
| 279 | superior frontal gyrus*† | 8 | 4 | 18 | 56 | 7.03 |
| 1357 | left inferior temporal gyrus* | 37 | -46 | -64 | -6 | 6.73 |
| 350 | cingulate gyrus* | 24 | 2 | 0 | 34 | 6.73 |
| 30 | left cerebellum* | -- | -26 | -72 | -32 | 4.85 |
| 21 | right middle frontal gyrus/superior orbital gyrus* | 11 | 22 | 34 | -18 | 4.40 |